Electronic Supplementary Material (ESI) for ChemComm.

Supplementary Information

Covalent Coupling via Dehalogenation on Ni(111) Supported Boron Nitride and Graphene

Claudius Morchutt,[ac] Jonas Björk,[b] Sören Krotzky,[a] Rico Gutzler[a] and Klaus Kern[ac]

[a] Max Planck Institute for Solid State Research, Heisenbergstrasse 1, 70569 Stuttgart, Germany.
[b] Department of Physics, Chemistry and Biology, IFM, Linköping University, 58183 Linköping, Sweden.
[c] Institut de Physique de la Matière Condensée, Ecole Polytechnique Fédérale de Lausanne, 1015 Lausanne, Switzerland.

Experimental Methods

STM data were acquired with etched tungsten tips (bias with respect to the sample) at room temperature. The samples used are crystalline Nickel films (typical thickness of 150 nm) on silicon substrates with an yttria-stabilized zirconia buffer layer. Further growth details can be found elsewhere.[1] The sample preparation consists of cleaning via Ar^+ sputtering (800 eV, 15 min) and annealing (750 °C, 15 min). A single layer of h-BN was grown by exposing the Ni surface held at 750 °C to 360 Langmuir of borazine ($B_3H_6N_3$).[2] A single film of graphene was grown by exposing the Ni surface held at 580°C to 225 Langmuir of ethylene (C_2H_4).[3]

Additional STM images

STM images of clean h-BN/Ni(111)

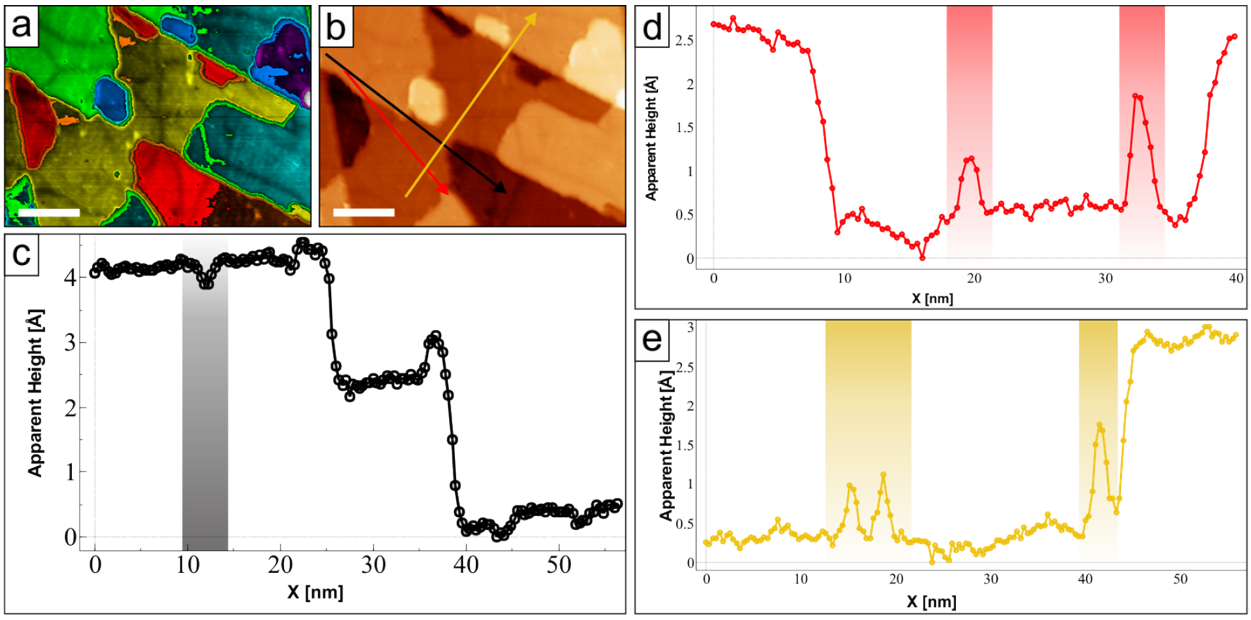

Figure S1 (a) and (b) STM data displayed with different colour coding of a clean h-BN/Ni(111) surface (scale bars: 15 nm). Typical domain boundaries of the h-BN layer are visible as darker, branched features on the terraces. (c) Linescan profile along the black line in (b). Monoatomic steps of about 2 Å height are observed. (d) and (e) Linescan profile along the red and yellow line, respectively, crossing several bright protrusions on the yellow coloured terrace. The height of these protrusions is < 2.0 Å, which is less than the step edge height. They are also smaller than the observed bright protrusions that appear after the polymerization reaction (compare Figs. S5 and S6), which consistently measure > 3.0 Å. The protrusions on the h-BN surface prior to molecule deposition are thus not of the same origin as the protrusions after the coupling reaction.

STM images of clean graphene/Ni(111) with atomic resolution

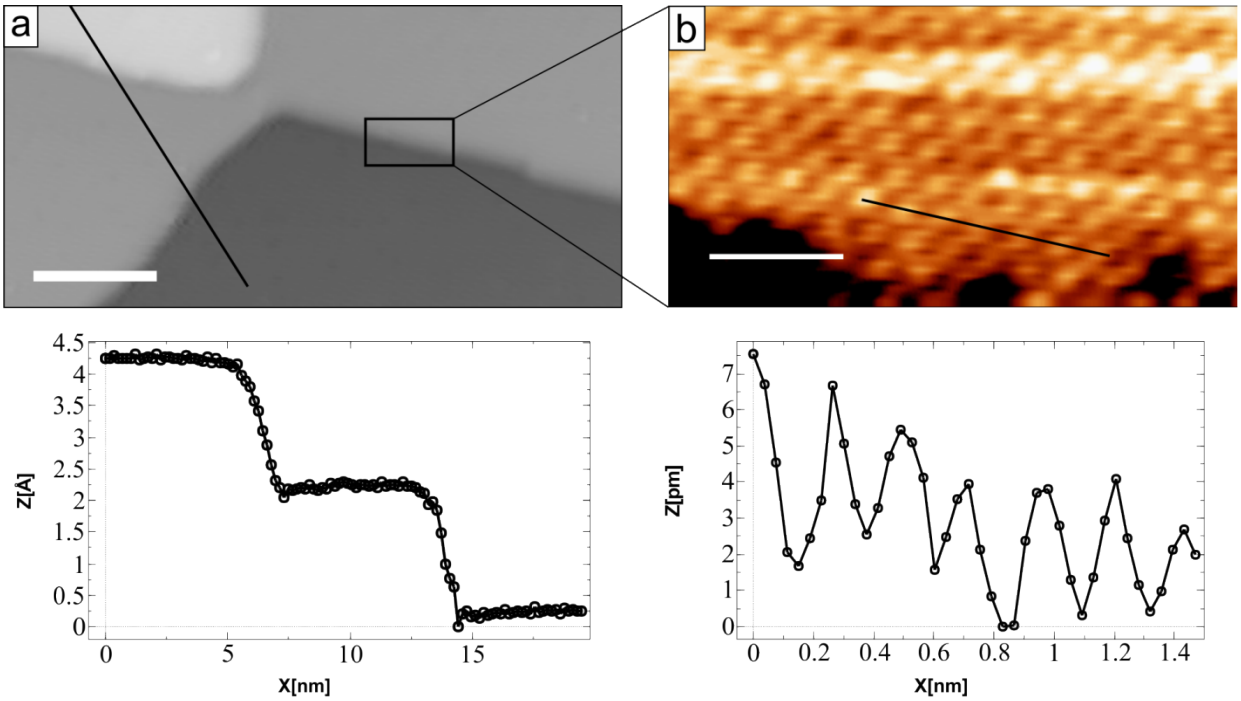

Figure S2 (a) STM image of the clean graphene/Ni(111) surface with a linescan profile along the black line. The terrace height is approximately 2 Å, the expected value for monoatomic step edges. No impurities are observable. (b) Zoom-in shows atomic resolution of the graphene layer. Linescan along the black line reveals a corrugation of approximately 2.5 Å which is in line with the nearest-neighbour distance of graphene on Ni (2.49 Å). Scale bar in (a): 6.3 nm, and in (b): 8.2 Å.

Successive annealing of TBB on bare Ni(111)

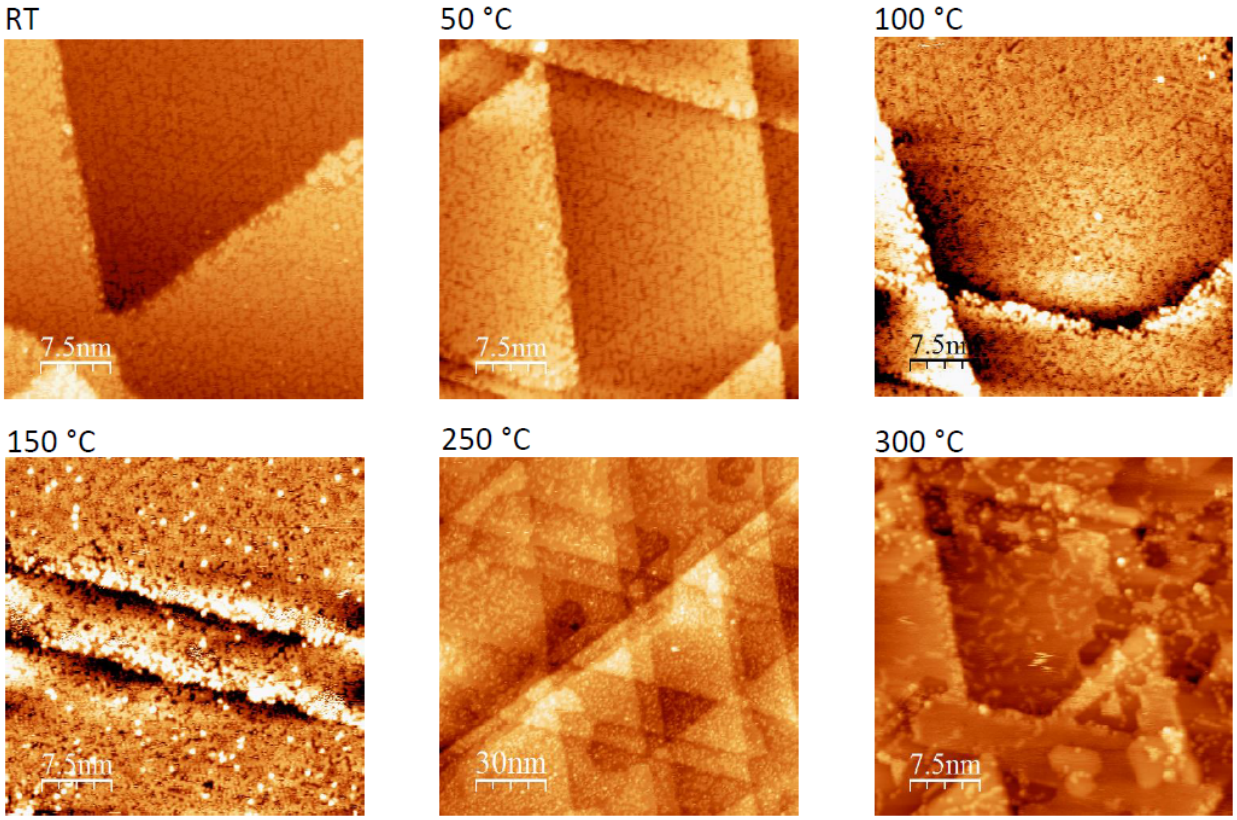

Figure S3 Successive annealing of TBB on bare Ni(111). Temperatures are shown above each panel. Decomposition and degradation of TBB monomers starts at 150 °C. No oligomers/polymers are observed. In the monolayer structure below 100 °C, no long-range order is observed.

Self-assembly of TBB on h-BN/Ni(111)

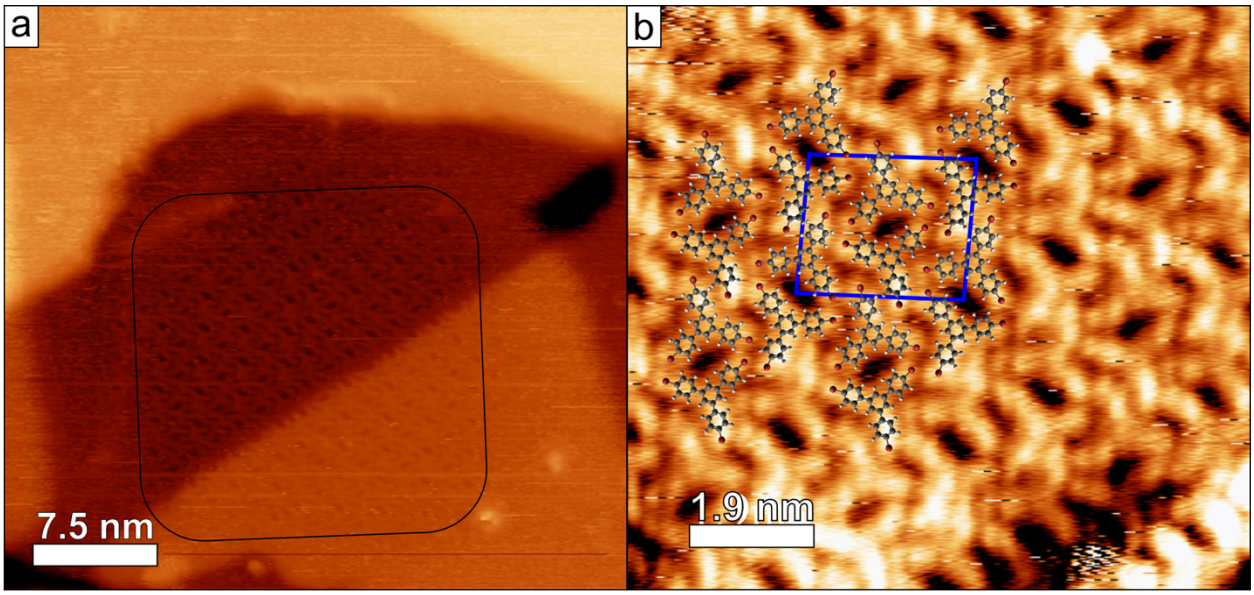

Figure S4 (a) Island of self-assembled TBB on h-BN/Ni(111) after deposition onto a hot surface (140 °C). The domain of about 340 nm^2 is surrounded by the bare h-BN/Ni(111) surface, where no self-assembly is observed. (b) Zoom-in on the self-assembled structure. Single molecules are revealed and a scaled ball-and-stick model of calculated dimers as described in the main text is superimposed. The unit cell is indicated in blue.

Intermolecular distances and apparent height

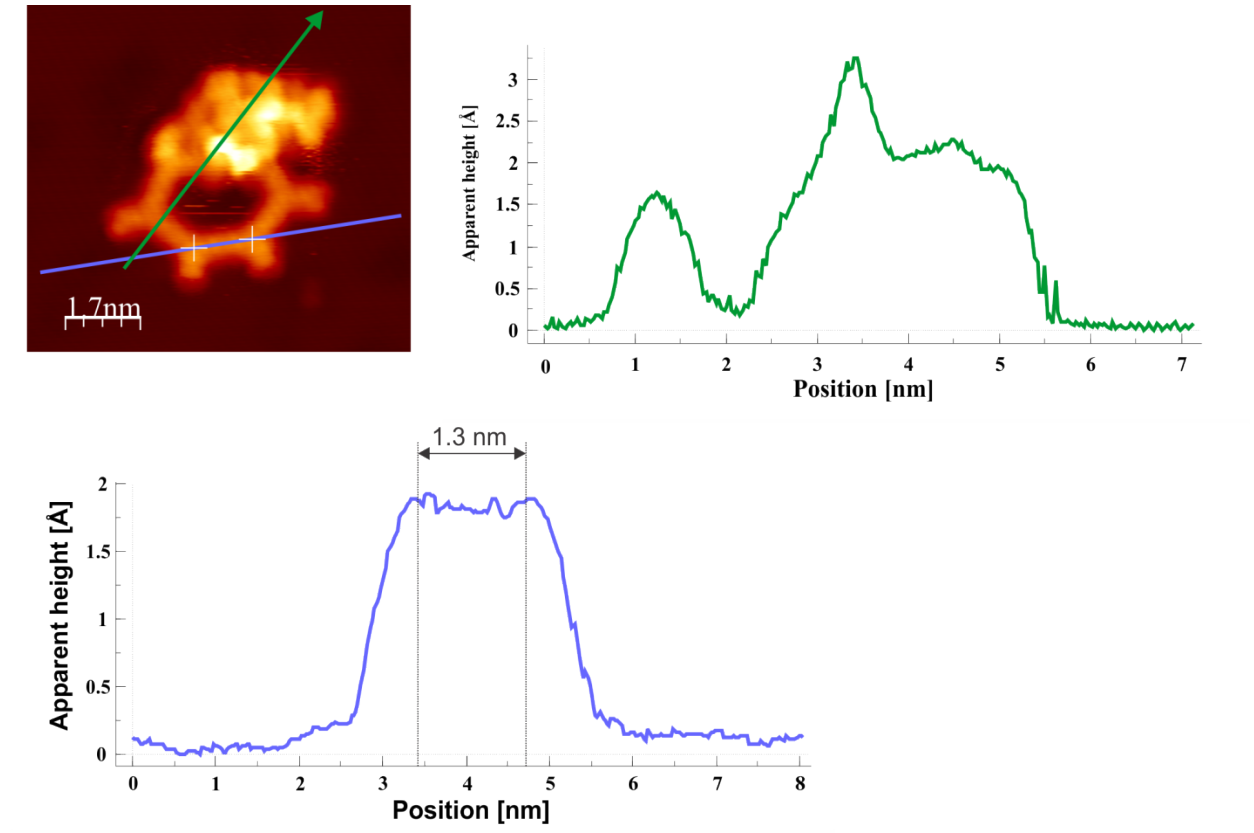

Figure S5 Linescans of a quasi-hexagon on h-BN/Ni(111). Top right: Apparent height of phenylene and a bright protrusion. The apparent height of the bright feature is about twice that of the oligomer. Bottom: Intermolecular distances of 1.3 nm confirm the formation of covalent bonds between monomers.

Linescan of overview STM image

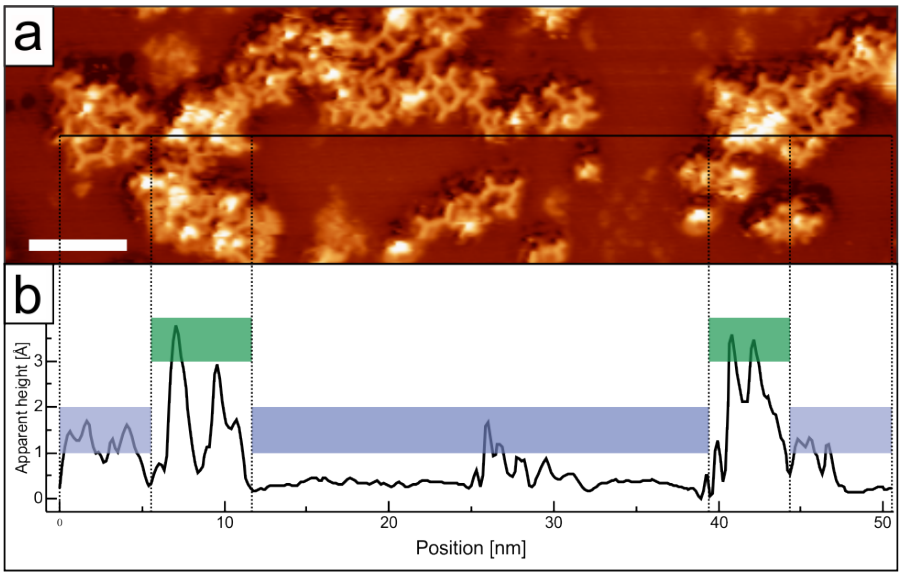

Figure S6 Linescan of oligomers formed on h-BN/Ni(111). The oligomers have an apparent height of ~1.5 Å, whereas bright protrusions show an apparent height of ~3.5 Å.

Self-assembly of TBB on graphene/Ni(111)

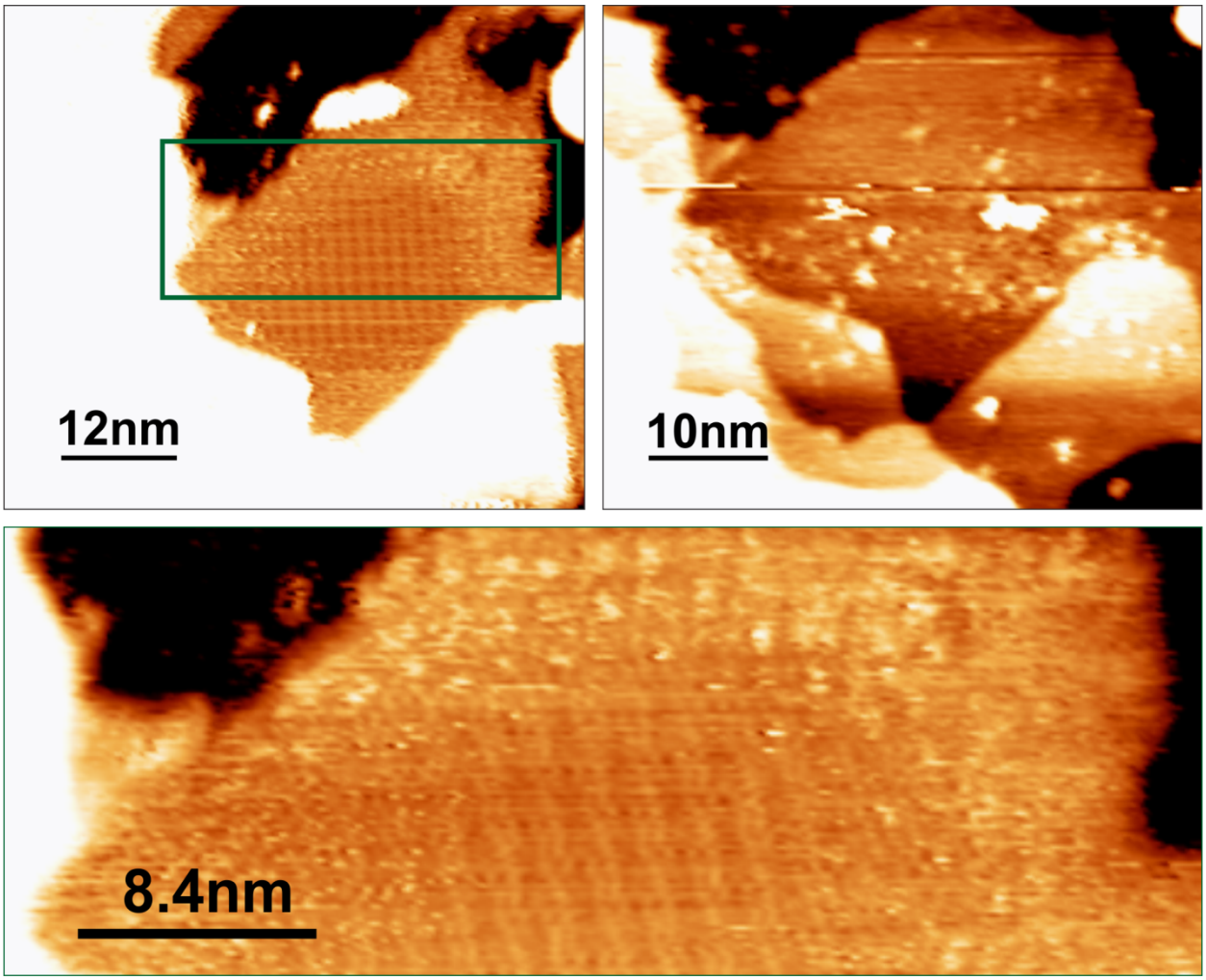

Figure S7 Self-assembly of TBB on graphene/Ni(111) after annealing at 100 °C for 15 minutes recorded at room temperature. Top right shows the same area applying small voltages pulses, resulting in the decomposition of the ordered structure.

Arrhenius plots

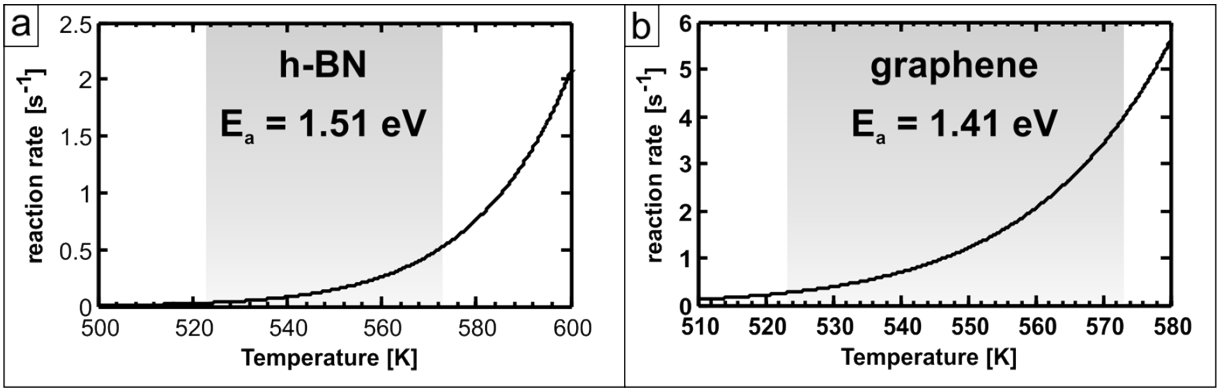

Figure S8 Arrhenius plots for debromination with barriers calculated for bromobenzene on (a) h-BN/Ni(111) and (b) graphene/Ni(111). The temperature range used in the experiments is highlighted in grey, and the rates were obtained assuming a pre-exponential factor of 10^{13} s^{-1}.

Computational details

The calculations were done within the framework of periodic density functional theory (DFT) with the VASP code,[4] using the projector-augmented wave method to describe ion-core interactions,[5] and the plane waves basis expanded to a kinetic energy cutoff of 500 eV. Exchange-correlation effects were described by the recent version of the van der Waals density functional (vdWDF)[6] introduced by Hamada[7] denoted as rev-vdWDF2, which makes use of the non-local correlation of vdWDF2[8] in combination with a revised form of Becke 86 exchange. This combination of exchange and correlation has shown to accurately describe both the graphene-Ni interface and the adsorption of different polycyclic aromatic hydrocarbons on a series of surfaces.[9] The Ni substrate was modeled by a four layered slab separated by a vacuum region of 20 Å, leaving enough room for the benzene/h-BN layer and adsorbed molecule. All atoms, except for the bottom two layers of the Ni slab, were structurally optimized until the forces acting on the atoms were smaller than 0.01 eV/Å. In all calculations except for the TBB radical, a surface unit cell of 6×6 together with a 3×3 k-point sampling was used. For the calculations of the TBB radical diffusion we used a surface unit cell of 9×9 using the Γ-point only to sample the 1st Brillouin zone. The experimental lattice constant for Ni of 3.524 Å was used throughout, as rev-vdWDF2 gives a slightly underestimated lattice constant that gives rise to buckling of h-BN for the extended cell. The choice of lattice constant of Ni does not affect the results, as shown for the dehalogenation on graphene-Ni, for which deviations below 50 meV are found for both energy barrier and reaction energy when using the experimental lattice parameter of Ni instead of the one obtained with rev-vdWDF2.

Both h-BN and graphene are known to form commensurate overlayers on Ni(111)[10], which is a result of matching lattice constants and a strong interaction with the Ni. In the case of h-BN/Ni(111), we found that in the most stable structure to be with the N on-top of Ni atoms and with the B in FCC hollow sites in accordance with previous theoretical[11] and experimental[12] studies. For graphene/Ni(111) we found that in the most stable structure one C-atom sits at a top-site while the other resides in a FCC hollow site, in agreement with previous experimental[13] and theoretical[14] studies.

Transition states were calculated using a combination of the climbing image nudged elastic band (CI-NEB)[15,16] and Dimer methods,[17,18] as described in Ref. [19]. For the CI-NEB calculations the number of images was adjusted specifically for each transition-state calculation such that the tangent along the path was well described, using typically 12−16 images. The CI-NEB method was used to find a rough estimate of the transition state. This estimate was then used to set up the starting configuration (central image and dimer) in the computationally much less demanding Dimer method. The structural optimizations of transition states were performed until the forces acting on the atoms on the central images, in the Dimer method, were smaller than 0.02 eV/Å.

Bromobenzene adsorption

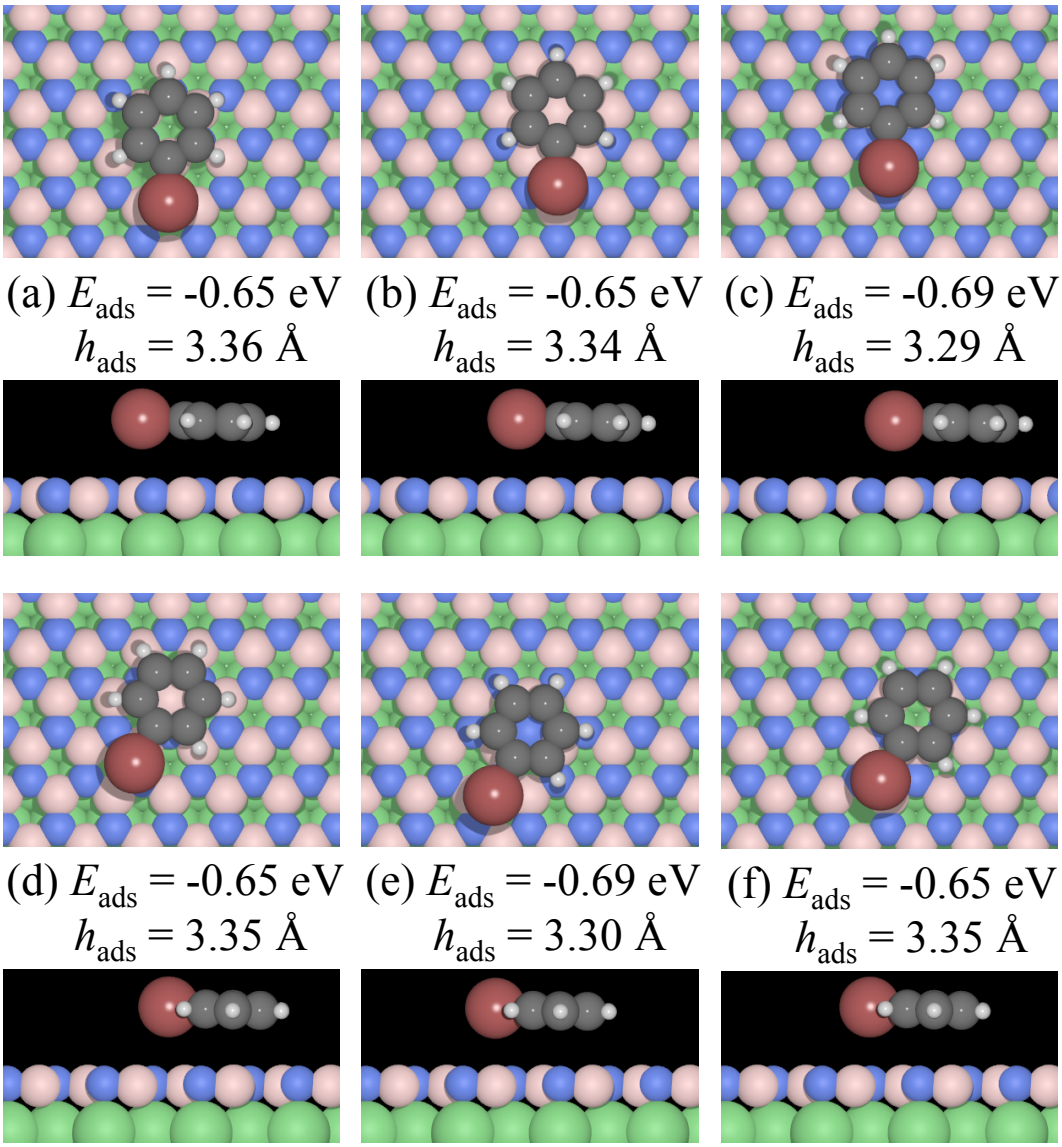

Figure S9 Adsorption configurations of bromobenzene on h-BN/Ni(111), with respective adsorption energies and average adsorption heights (above the h-BN layer) indicated.

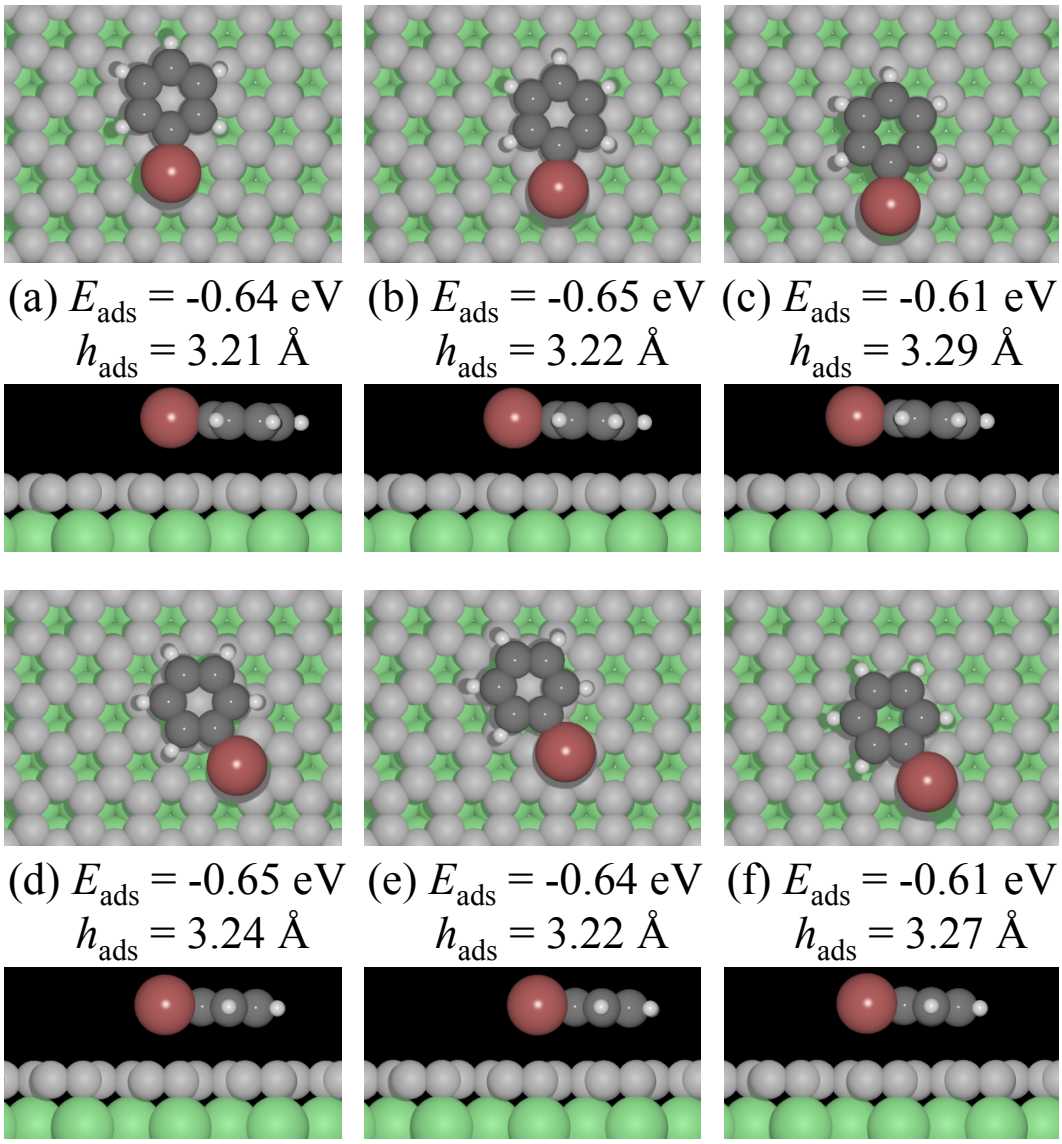

Figure S10 Adsorption configurations of bromobenzene on graphene/Ni(111), with respective adsorption energies and average adsorption heights (above the graphene layer) indicated.

Phenyl radical adsorption

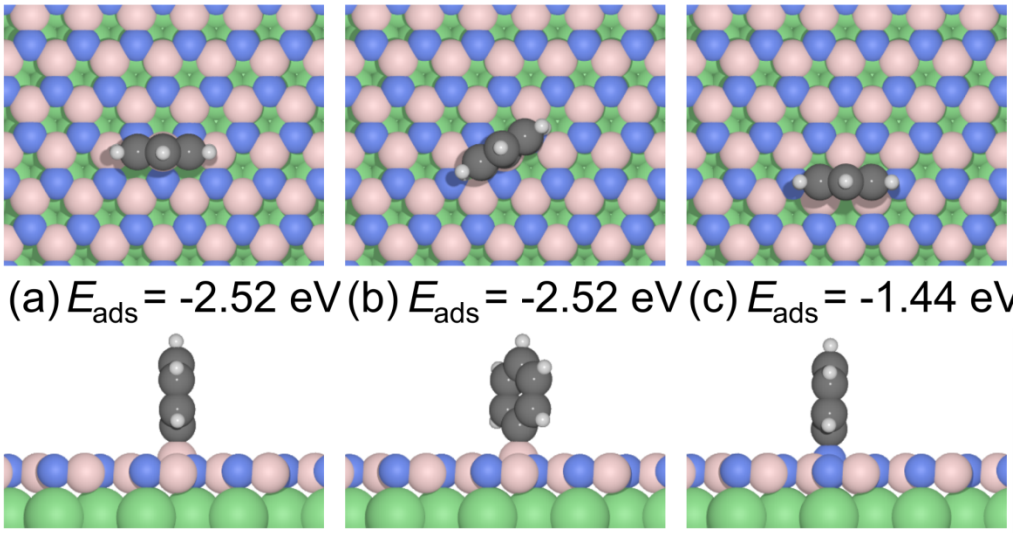

Figure S11 Top and side views of different adsorption geometries of a phenyl radical adsorbed on h-BN/Ni(111), with respective adsorption energies indicated, calculated with respect to the clean h-BN/Ni(111) surface and phenyl radical in gas phase.

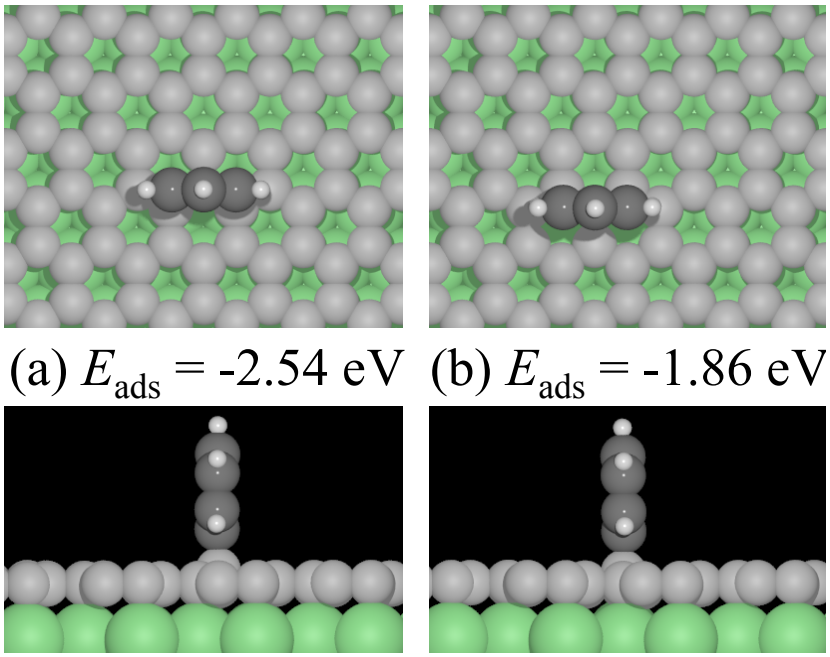

Figure S12 Top and side views of different adsorption geometries of a phenyl radical adsorbed on graphene/Ni(111), with respective adsorption energies indicated, calculated with respect to the clean graphene/Ni(111) surface and phenyl radical in gas phase.

Bromine atom adsorption

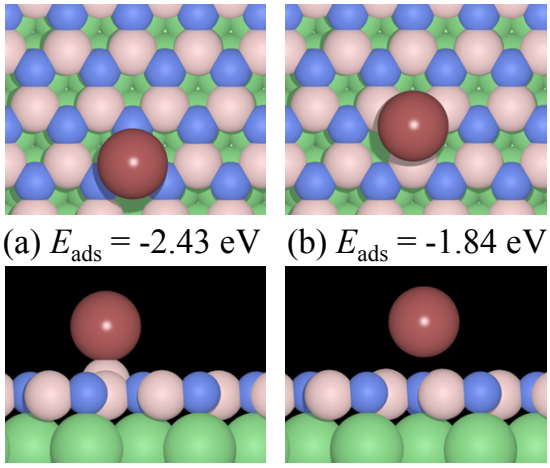

Figure S13 Top and side views of different adsorption configurations of a bromine atom adsorbed on h-BN/Ni(111), with respective adsorption energies indicated, calculated with respect to the clean h-BN/Ni(111) surface and a bromine atom gas phase.

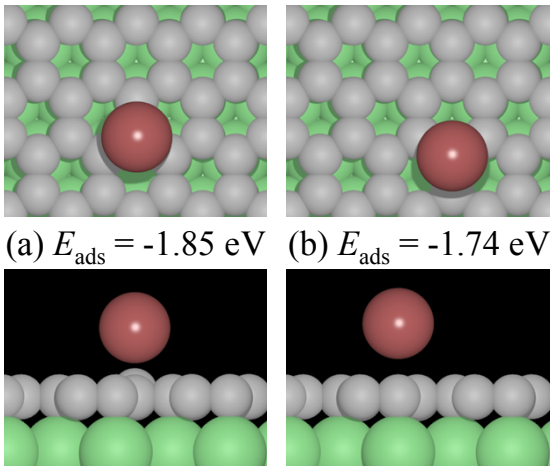

Figure S14 Top and side views of different adsorption geometries of a bromine atom adsorbed on graphene/Ni(111), with respective adsorption energies indicated, calculated with respect to the clean graphene/Ni(111) surface and bromine atom in gas phase.

Phenyl radical diffusion on h-BN/Ni(111)

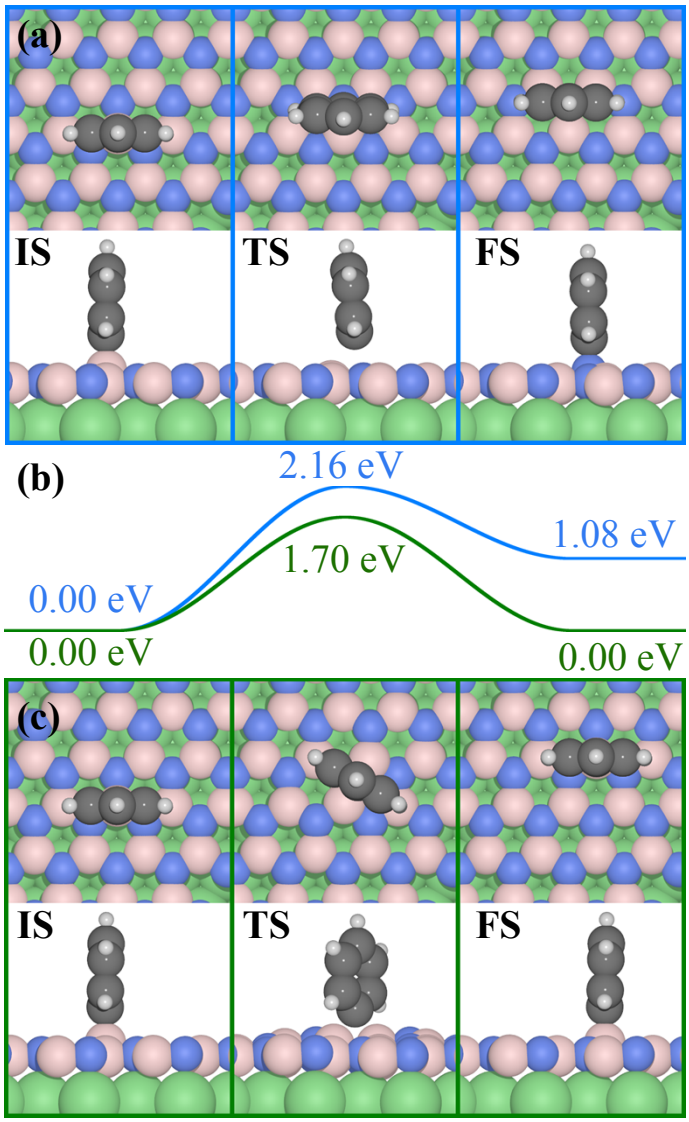

Figure S15 (a,c) Initial state (IS), transition state (TS) and final state (FS) for two different diffusion paths of phenyl on h-BN/Ni(111). (b) Energy diagram of the two paths with the path in (a) in blue and the path in (c) in green.

TBB radical diffusion on h-BN/Ni(111)

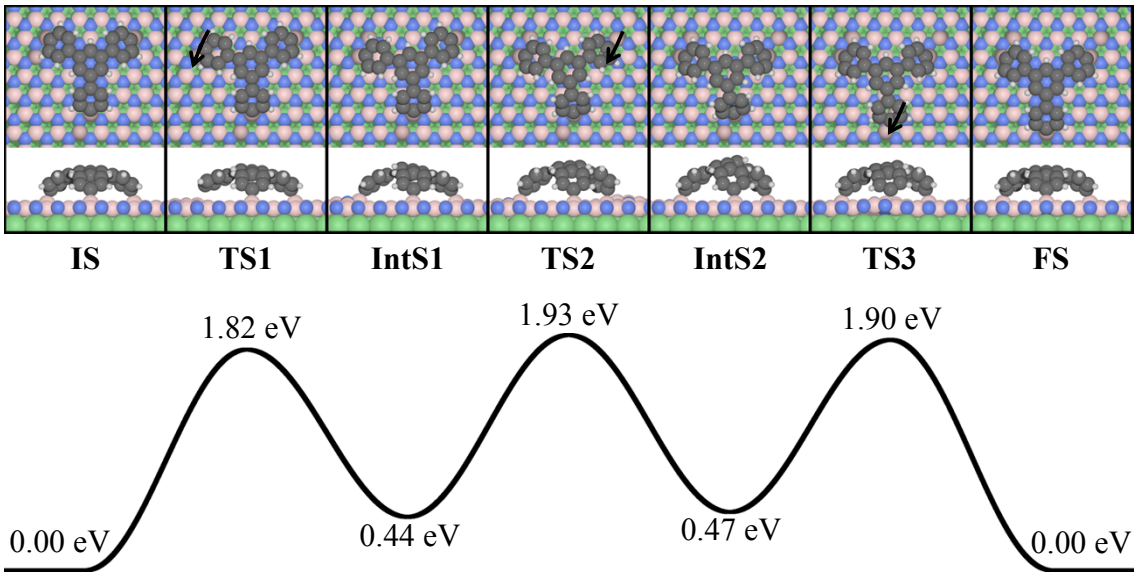

Figure S16 TBB radical diffusion. The molecule needs to climb at least three subsequent barriers, moving one phenyl leg at a time, to go between two equivalent B adsorption sites on the surface. Each of these steps has a barrier of ~1.9 eV.

Dehalogenation of bromobenzene on single-sheet graphene (no Ni(111) support)

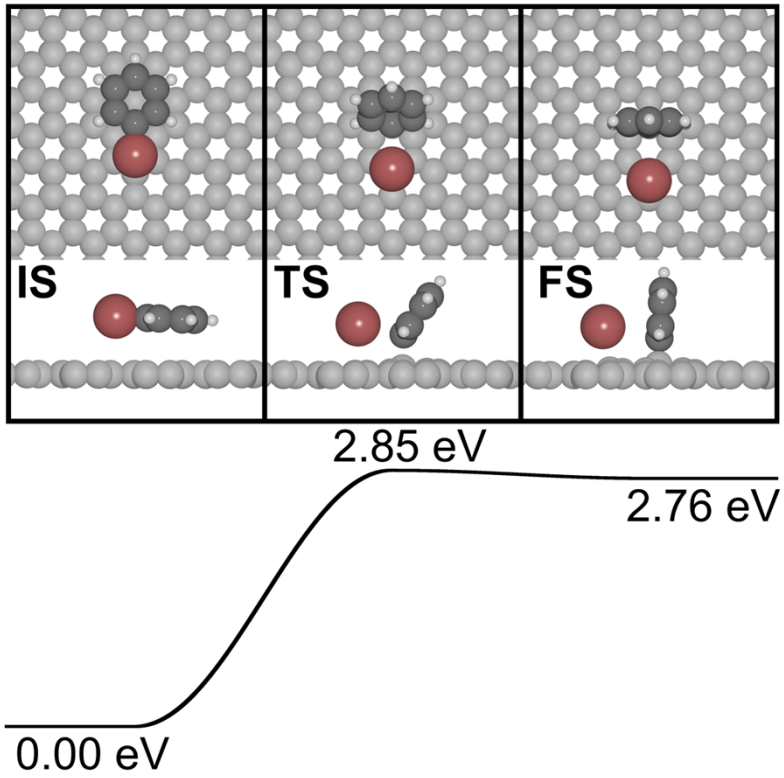

Figure S18 Dehalogenation of bromobenzene on free-standing graphene. The reaction is strongly endothermic and the reaction barrier (2.85 eV) is significantly larger compared to the reaction on Ni supported graphene.

Dehalogenation of bromobenzene on single-sheet h-BN (no Ni(111) support)

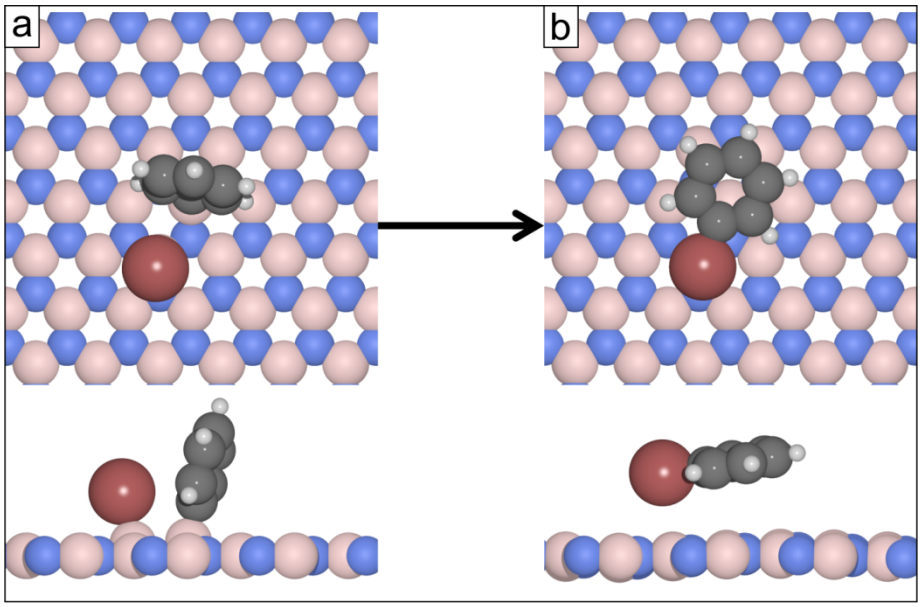

Figure S19 The transition state (a) of the debromination calculated for h-BN/Ni(111) is unstable once the Ni(111) substrate is removed. During geometry optimization, the molecule reassembles and relaxes into the initial state of an intact molecule (b). In absence of Ni(111), h-BN shows no catalytic activity for debromination.

References

1. S. Gsell, M. Fischer, M. Schreck, and B. Stritzker, *J. Cryst. Growth*, 2009, **311**, 3731–3736.

2. W. Auwärter, M. Muntwiler, J. Osterwalder, and T. Greber, *Surf. Sci.*, 2003, 545, L735–L740.

3. J. Lahiri, T. S Miller, A. J Ross, L. Adamska, I. I. Oleynik, and M. Batzill, *New J. Phys.*, 2011, **13**, 025001.

4. G. Kresse, *Phys. Rev. B*, 1996, 54, 11169–11186.

5. P. E. Blöchl, *Phys. Rev. B*, 1994, **50**, 17953–17979.

6. M. Dion, H. Rydberg, E. Schröder, D. C. Langreth, and B. I. Lundqvist, *Phys. Rev. Lett.*, 2004, **92**, 246401–1.

7. I. Hamada, *Phys. Rev. B*, 2014, **89**, 121103.

8. K. Lee, É. D. Murray, L. Kong, B. I. Lundqvist, and D. C. Langreth, *Phys. Rev. B*, 2010, **82**, 081101.

9. J. Björk and S. Stafström, *ChemPhysChem*, 2014, **15**, 2851–8.

10. C. Oshima and A. Nagashima, *J. Phys. Condens. Matter*, 1997, **9**, 1–20.

11. A. H. M. A. Wasey, S. Chakrabarty, G. P. Das, and C. Majumder, *ACS Appl. Mater. Interfaces*, 2013, **5**, 10404–8.

12. M. Muntwiler, W. Auwärter, F. Baumberger, M. Hoesch, and J. Osterwalder, *Surf. Sci.*, 2001, **472**, 125–132.

13. Y. Gamo, A. Nagashima, M. Wakabayashi, M. Terai, and C. Oshima, *Surf. Sci.*, 1997, **374**, 61–64.

14. F. Mittendorfer, a. Garhofer, J. Redinger, J. Klimeš, J. Harl, and G. Kresse, *Phys. Rev. B*, 2011, **84**, 201401.

15. G. Henkelman and H. Jónsson, *J. Chem. Phys.*, 2000, **113**, 9978–9985.

16. G. Henkelman, B. P. Uberuaga, and H. Jónsson, *J. Chem. Phys.*, 2000, **113**, 9901–9904.

17. G. Henkelman and H. Jónsson, *J. Chem. Phys.*, 1999, **111**, 7010–7022.

18. J. Kästner and P. Sherwood, *J. Chem. Phys.*, 2008, **128**, 014106.

19. J. Björk, F. Hanke, and S. Stafström, *J. Am. Chem. Soc.*, 2013, **135**, 5768–5775.